

## Initial phase wall conditioning in KSTAR

Suk-Ho Hong<sup>1,2,†</sup>, Kwang-Pyo Kim<sup>1</sup>, Kyung-Min Kim<sup>1</sup>, Kun-Su Lee<sup>1</sup>, Sung-Woo Kim<sup>1</sup>, Dong-Su Lee<sup>1</sup>, Sun-Ho Kim<sup>4</sup>, Jong-Su Kim<sup>1</sup>, Sun-Jung Wang<sup>4</sup>, Jong-Ho Sun<sup>2,3</sup>, Hyun-Jong Woo<sup>2,3</sup>, Jae-Min Park<sup>1</sup>, Woong-Chae Kim<sup>1</sup>, Hak-Kun Kim<sup>1</sup>, Kap-Rae Park<sup>1</sup>, Jong-Gu Kwak<sup>4</sup>, Hyung-Lyeol Yang<sup>1</sup>, Yeong-Kook Oh<sup>1</sup>, Hoon-Kyun Na<sup>1</sup>, Kyu-Sun Chung<sup>2,3</sup>, and KSTAR team<sup>1</sup>

<sup>1</sup>*National Fusion Research Institute, 113 Gwahangno, Yuseong-Gu, Daejeon, 305-333, Korea*

<sup>2</sup>*Center for Edge Plasma Science (cEps), Hanyang University, Seoul 133-791, Korea.*

<sup>3</sup>*Department of Electrical Engineering, Hanyang University, Seoul 133-791, Korea.*

<sup>4</sup>*Korea Atomic Energy Research Institute, Daejeon, , Korea*

**Abstract** Initial phase wall conditioning in KSTAR is depicted. The KSTAR wall conditioning procedure consists of baking, Glow Discharge Cleaning (GDC), ICRH Wall Conditioning (ICWC), and boronization (Bz). The vessel baking has been performed in order to remove various kinds of impurities including H<sub>2</sub>O, carbon and oxygen for the plasma. The total outgassing rates in the KSTAR campaigns are compared. GDC is regularly performed as standard wall cleaning procedure. Another cleaning technique is ICWC, which is useful for inter-shot wall conditioning under strong magnetic field. In order to optimize operation time and removal efficiency, parameter scan has been performed. Bz is a standard technique to remove oxygen impurity from vacuum vessel. KSTAR has utilized carborane powder which is non-toxic boron containing material. The first bz has been performed successfully. Water and oxygen level in vacuum vessel have been reduced significantly. Boron containing thin films deposited by boronization are studied.

### 1. Introduction

A good initial vacuum and wall conditioning procedure is essential to obtain high-quality wall condition for plasma experiments. Various kinds of wall conditioning techniques have been utilized to remove impurities from the surface of Plasma Facing Components (PFCs) including H<sub>2</sub>O, carbon and oxygen compounds [1].

At first, the vacuum vessel of a tokamak is baked after a long vent for maintenance. Baking operation depends not only on the baking temperature and duration, but also several factors such as capability of the baking system, wall material, and maximum heat load limitation of installed diagnostic/wall components. DC Glow Discharge Cleaning (GDC) is applied simultaneously or sequentially to enhance the cleaning efficiency [2]. Because GDC doesn't work under permanent magnetic fields produced by superconducting magnets, GDC cannot be operated as an inter-shot wall conditioning method for superconducting (future) tokamak like KSTAR (Korea Superconducting Tokamak Advanced Research) and ITER (International Thermonuclear Experimental Reactor): Another wall conditioning technique such as Ion Cyclotron Wall Conditioning (ICWC) or Electron Cyclotron Wall Conditioning (ECWC) is essential. Many machines have reported that ICWC plasmas have been generated successfully in a wide range of frequency range from 10 to 100 MHz [3].

Boronization in a Glow Discharge (GD) is a standard and widely applied technique to remove oxygen impurity from a vacuum vessel. In general, B<sub>2</sub>H<sub>6</sub> (B<sub>2</sub>D<sub>6</sub>) gas is used to deposit boron containing thin films on the wall that have excellent oxygen gettering functionality [1].

The aim of the paper is to report briefly the initial wall conditioning procedures and results in KSTAR. The paper is organized as follows. In section 2, we will shortly describe the

---

<sup>†</sup> email: [sukhhong@nfri.re.kr](mailto:sukhhong@nfri.re.kr)

experimental setup, i.e., the baking system, GDC system, ICWC system, boronization system, and the wall conditioning procedures. In section 3, the results of each wall conditioning method are discussed. Finally, summary and conclusion will be given.

## 2. Experimental Setup and Procedures

KSTAR has accomplished its construction in 2007. The KSTAR is a medium size tokamak which have a major radius of 1.8 m, a minor radius of 0.5 m, a maximum toroidal field strength of 3.5 teslas (T), and a maximum plasma current of 2 MA. Heating and current drive system will be Neutral Beam Injection (NBI), Ion Cyclotron Resonance Heating (ICRH), Electron Cyclotron Resonance Heating (ECRH). The KSTAR is upgraded for the 3<sup>rd</sup> campaign with its new target mission to produce the D-shaped plasma with a target plasma current of 500 kA and/or pulse length of 5 seconds.

### 2.1. Baking

The aim of the baking is to remove impurities from the surface of vacuum vessel, PFCs, pumping duct, and in-vessel components. Thus, these components have to be baked at a proper temperature. Since KSTAR has been upgraded through the campaigns, the baking system is also gradually upgraded: Vacuum vessel baking system (1<sup>st</sup> campaign), jacket heaters for pumping duct (2<sup>nd</sup> campaign), hot nitrogen baking system for PFCs (3<sup>rd</sup> campaign). The baking temperature was 100°C to 225 °C for several days.

### 2.2. Glow Discharge Cleaning

The KSTAR GDC system has two reciprocating-type movable RF antennas at port A and I. At the end of the antennas, 10-turn induction coil was utilized to launch 300 W RF power at a frequency of 13.56 MHz to produce initial breakdown [3]. The antennas are located at the outside of ports while plasma experiments are performed, and positioned at the center of vacuum vessel for GDC. After the breakdown, DC bias is applied between the antenna and the vacuum vessel at 200-500 V and 2 kW. H<sub>2</sub>/D<sub>2</sub> or He GDCs are regularly performed through the campaigns, usually at night.

### 2.3. ICRF Wall Conditioning

The KSTAR ICRF antenna consists of four current straps covered with Faraday shield. It is powered by 2 MW RF transmitter through vacuum transmission line, pressurized resonant loop and double liquid stub tuner [4]. Two poloidal limiters are attached at both sides of the ICRH antenna. For ICWC experiment, second and third current straps are driven with 0-pi phasing corresponding to  $k_{\parallel} = 16 \text{ m}^{-1}$  and the power about 20kW to 50kW is applied at pulse or CW mode. The driving frequency is 44.2 MHz which is selected for minority D(H) heating at 3T. The resonance layer is located at  $r=1.8 \text{ m}$ .

### 2.4. Boronization

KSTAR boronization is based on a carborane (C<sub>2</sub>B<sub>10</sub>H<sub>12</sub>) injection system. The technique is widely used in Russian tokamaks [5] and HT-7, and EAST [6]. Carborane solid powder is

heated up to 120 °C in a dedicated evaporator oven located outside the KSTAR cryostat. Through a guiding pipe system, evaporated hot carborane vapor is introduced into the vacuum vessel. In order to avoid the re-condensation of carborane inside the pipe, the temperature of the pipe was also controlled and heated up to 120 °C. The flow rate of carborane is controlled by oven temperature and a gate valve. A detailed description of the system can be found in a publication [7]. Boronization in KSTAR is a three-step procedure: 1) 2 hours of He glow discharge conditioning (GDC) is performed to clean the walls. 2) carborane is injected into a pulsed He GD to produce boron containing thin films. 3) after the boronization, walls are saturated by H atoms dissociated from carborane molecules. Thus, 1-2 hour of He GDC is performed to desaturate H from the walls. The quality of the deposited films was measured by ex-situ diagnostics (see below).

### 3. Results and Discussion

In this section, we will describe the wall conditioning results in detail. Different techniques were performed simultaneously or sequentially.

#### 3.1. Baking

Outgassing rate (leak rate) of an isolated vacuum system is defined as

$$Q = V \times \frac{\Delta P}{\Delta t} \quad (1)$$

where  $Q$ ,  $V$ ,  $\Delta P$ , and  $\Delta t$  are the total outgassing rate, the volume of the vacuum chamber, the pressure difference in the vacuum vessel, and the time interval, respectively. Table 1 shows the measured outgassing rates through three campaigns from 2008 to 2010. Total outgassing rate increases campaign by campaign as the surface area of PFCs in the vacuum vessel increases: The outgassing rate in the KSTAR 3<sup>rd</sup> campaign is a factor of 4.5 larger than that in the KSTAR 1<sup>st</sup> campaign. However, the outgassing rate per unit area is decreased due to the upgrade of the baking system. This indicates that the baking system is proven to be effective in removing impurities.

Item	1 <sup>st</sup> campaign	2 <sup>nd</sup> campaign	3 <sup>rd</sup> campaign
PFCs Surface area (m <sup>2</sup> )	1.54	11	54
Outgassing rates (mbar·ℓ·s <sup>-1</sup> )	1.43 × 10 <sup>-4</sup> (M <sub>28</sub> dominated)	1.93 × 10 <sup>-4</sup> (M <sub>2</sub> dominated)	6.49 × 10 <sup>-4</sup> (M <sub>28</sub> dominated)
Per unit area (mbar·ℓ·m <sup>-2</sup> ·s <sup>-1</sup> )	9.31 × 10 <sup>-5</sup>	1.75 × 10 <sup>-5</sup>	1.20 × 10 <sup>-5</sup>

Table 1: Outgassing rates measured after the baking operation in 2008-2010 KSTAR campaigns.

Table 2 shows outgassing rates of major impurities in the KSTAR 3<sup>rd</sup> campaign. The most dominant gas species in the vacuum vessel are M<sub>18</sub> before baking, M<sub>44</sub> after the 1<sup>st</sup> baking, and M<sub>28</sub> after the 2<sup>nd</sup> baking, respectively. M<sub>18</sub> (H<sub>2</sub>O) decreased from 1.91 × 10<sup>-3</sup> mbar·ℓ·s<sup>-1</sup> to

$1.25 \times 10^{-5} \text{ mbar} \cdot \ell \cdot \text{s}^{-1}$  after the baking operation. However,  $M_2$  (Hydrogen) increased from  $6.17 \times 10^{-5} \text{ mbar} \cdot \ell \cdot \text{s}^{-1}$  to  $1.33 \times 10^{-4} \text{ mbar} \cdot \ell \cdot \text{s}^{-1}$  due to the increasing number of hydrogen particles detached from the surface/bulk of PFCs by the hot nitrogen baking (maximum temperature at  $225^\circ \text{C}$ ).

Outgassing rate ( $\text{mbar} \cdot \ell \cdot \text{s}^{-1}$ )	Before baking	1 <sup>st</sup> baking (Tem. $125^\circ \text{C}$ )	2 <sup>nd</sup> baking (Tem. $225^\circ \text{C}$ )
$M_2$	$6.17 \times 10^{-5}$	$6.17 \times 10^{-4}$	$1.33 \times 10^{-4}$
$M_{18}$	$1.91 \times 10^{-3}$	$6.38 \times 10^{-5}$	$1.25 \times 10^{-5}$
$M_{28}$	$1.15 \times 10^{-3}$	$7.06 \times 10^{-4}$	$3.99 \times 10^{-4}$
$M_{44}$	$1.15 \times 10^{-3}$	$8.04 \times 10^{-4}$	$8.39 \times 10^{-5}$
Total	$4.64 \times 10^{-3}$	$1.69 \times 10^{-3}$	$6.49 \times 10^{-4}$
Per unit area ( $\text{mbar} \cdot \ell \cdot \text{m}^{-2} \cdot \text{s}^{-1}$ )	$8.58 \times 10^{-5}$	$3.12 \times 10^{-5}$	$1.22 \times 10^{-5}$

Table 2: Outgassing rates of major impurities during the baking operation in the 3<sup>rd</sup> KSTAR campaign.

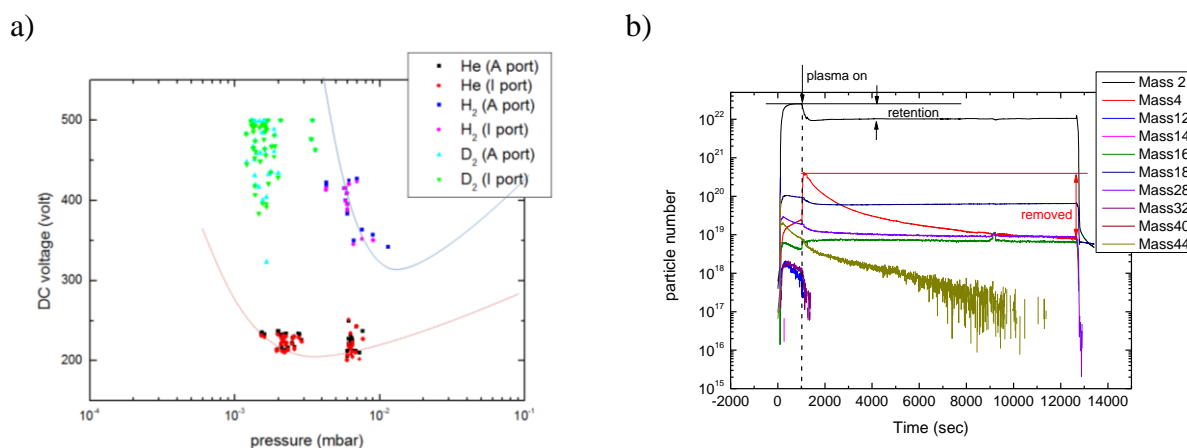


Figure 1. a) DC voltage as a function of pressure which is equivalent to Paschen's curve. b) particle number of H<sub>2</sub> GDC with pumping speed of 2800 l/s as an example. Label "plasma on" indicates when the input power is coupled. Labels "retention" and "removed" are for Table 3.

### 3.2. GDC

Operational windows have been scanned by varying pressure in the vacuum vessel and measuring DC voltage as shown in figure 1 a). The pressure range was changed from  $1.5 \times 10^{-3} \text{ mbar}$  to  $1.15 \times 10^{-2} \text{ mbar}$ , and coupled power was about 2.7 kW for H<sub>2</sub> and 1.7 kW for He with  $I_{\text{DC}} = 7 \text{ A}$ . The pumping speed was 11200 l/s (4 TMPs). In the case of He GDC, DC voltage does not depend much on the pressure difference indicating that the condition is around the Paschen's minima. On the other hand, the DC voltage drops about 100 V in H<sub>2</sub> GDC as the pressure in the vessel increases, meaning the condition has to be optimized towards higher pressure. In the case of D<sub>2</sub> GDC, the DC voltage is scattered in a broad range from 300 V up to 500 V. This reveals that the DC voltage of D<sub>2</sub> GDC would be affected sensitively by the vessel wall conditions while H<sub>2</sub> and He GDCs not. This makes the GDC start up difficult at the beginning of the 3<sup>rd</sup> campaign. Due to the "dirty" surface condition of the antenna at I port and that of newly installed in-vessel components, D<sub>2</sub> GDC was not stable

at I port due to too frequent arcs. In order to avoid the damage of the antenna and power supply, we have gradually increased the current from 1 A to 7 A in several hours.

Figure 1b) shows typical trend during H<sub>2</sub> GDC. As the RF input power is coupled, the plasma is generated (label: plasma on). H<sub>2</sub> pressure decreases due to the ionization and retention on the wall. The effect of H<sub>2</sub> GDCs at a pressure about  $4 \times 10^{-3}$  mbar is shown in Table 3. H<sub>2</sub> flow rate is regulated in order to match the pressure in the vacuum vessel (300 sccm for 1 TMP, 500 sccm for 2 TMPs). Direct comparison of the removed particles in Table 3 seems that the longer residence time (smaller pumping speed) results a better removal rate. A longer residence time results a longer reaction time at the surface of PFCs, and reionization, dissociation, recycling of released molecules in the plasma. Thus more H<sub>2</sub> particles are consumed and more impurities are released. However, the consequence of insufficient pumping speed brings the increase of the particle number (e.g., M<sub>18</sub> (H<sub>2</sub>O) and M<sub>16</sub>). Negative sign of M<sub>16</sub> indicates the increase of methane number density during H<sub>2</sub> GDC.

pumping speed (l/s)	H <sub>2</sub> flow rate (sccm)	M <sub>2</sub> (in plasma & retention)	M <sub>4</sub>	M <sub>16</sub>	M <sub>18</sub>	M <sub>28</sub>	M <sub>32</sub>	M <sub>44</sub>
2800	300	$4.55 \times 10^{20}$	$6.51 \times 10^{19}$	$-1.16 \times 10^{17}$	$3.32 \times 10^{18}$	$1.23 \times 10^{18}$	$3.98 \times 10^{17}$	$9.52 \times 10^{17}$
5600	500	$1.08 \times 10^{20}$	$3.50 \times 10^{19}$	$-4.49 \times 10^{17}$	$1.18 \times 10^{18}$	$2.71 \times 10^{17}$	$2.21 \times 10^{17}$	$4.28 \times 10^{17}$

Table 3. Removed particle number (removal rate: particles/sec) depending on the residence time during H<sub>2</sub> GDC. Pressure in both cases was about  $4 \times 10^{-3}$  mbar.

The effect of residence time on He GDCs at a pressure about  $6 \times 10^{-3}$  mbar is shown in Table 4. He flow rates are 750 sccm for 1 TMP, 1400 sccm for 2 TMPs, and 2100 sccm for 3 TMPs. Cleaning duration was about 334 min, 240 min, and 180 min, respectively. As we have seen from figure 1, the DC voltage for He GDC is almost the same indicating that the ion energy impinging on the surface does not vary much, but the residence time of gas species leads to a different plasma chemistry in the vacuum vessel. Overall removal rate shows that M<sub>2</sub> removal rate is the highest with two TMPs. Other masses show also higher removal efficiency with two TMPs. One TMP shows better removal rate than three TMP for H<sub>2</sub>. Positive sign of M<sub>16</sub> indicates that produced methane is properly removed.

Pumping speed (l/s)	He flow rate (sccm)	M <sub>2</sub>	M <sub>4</sub> (in plasma & retention)	M <sub>16</sub>	M <sub>18</sub>	M <sub>28</sub>	M <sub>32</sub>	M <sub>44</sub>
2800	750	$1.36 \times 10^{19}$	$1.49 \times 10^{21}$	$2.94 \times 10^{18}$	$2.53 \times 10^{18}$	$1.07 \times 10^{18}$	$2.77 \times 10^{17}$	$1.51 \times 10^{18}$
2800	950	$2.73 \times 10^{18}$	$6.19 \times 10^{20}$	$-2.24 \times 10^{17}$	$6.45 \times 10^{17}$	$2.16 \times 10^{17}$	$2.31 \times 10^{17}$	$4.51 \times 10^{16}$
5600	1400	$2.04 \times 10^{19}$	$1.48 \times 10^{20}$	$5.23 \times 10^{17}$	$2.64 \times 10^{17}$	$2.39 \times 10^{17}$	$2.66 \times 10^{17}$	$4.30 \times 10^{17}$
8400	2100	$3.65 \times 10^{18}$	$4.42 \times 10^{19}$	$2.46 \times 10^{17}$	$1.57 \times 10^{16}$	$-3.03 \times 10^{16}$	$-4.33 \times 10^{17}$	$1.81 \times 10^{17}$

Table 4. Removed particle number (removal rate: particles/sec) depending on pumping speed during He GDC. Pressure in three cases was about  $6 \times 10^{-3}$  mbar.

### 3.3. ICWC

A two-day dedicated session was planned for the ICWC parameter scan and fuel removal rate at a magnetic field of 3 T. To have an identical initial wall condition, 2 hour-D<sub>2</sub> night GDCs

were carried out to get  $D_2$  saturated wall. Various ICWC parameters have been scanned: Pressure (He/ $H_2$  mixture rate) and power coupling (CW, duty cycle). The response of the wall to the RF plasma is measured by RGA signals and emission spectroscopy. In addition to the dedicated session, inter-shot ICWC has been performed regularly during the campaign. Note that, because the TF field of the plasma shots was 2 T, no resonance layer was present during the inter-shot ICWC. Figure 2 a) shows masses  $H_2$  and HD depending on the  $H_2$  mixture rate. By using a night  $D_2$  GDC, The wall was saturated by  $\sim 10^{24}$  D atoms (similar to TS [9]). As He/ $H_2$  ICWC is performed, the isotope exchange has occurred. The retention of H increases, HD release increases. As the wall is saturated by H at 80 sccm, the H retention starts to decrease, thus production of HD decreases, too. The number of  $H_{\text{implanted}}$  is an order of  $\sim 10^{21}$ , while that of  $D_{\text{pumped}}$  is  $\sim 10^{20}$  with a ratio of  $H_{\text{implanted}}/D_{\text{pumped}} \sim 5-15$ . The H retention rate is of the order of  $\sim 10^{19}$  H/sec. Similarly, Tore Supra has reported the H retention rate of about  $3 \times 10^{19}$  H/sec with no sign of saturation [10], in TEXTOR about  $1-2 \times 10^{20}$  H/sec with a slight sign of saturation [10]. Note that, we cannot separate  $D_2$  and He by RGA. Nevertheless, the ICWC results from Tore Supra have shown that the  $D_2$  partial pressure during the He/ $H_2$  ICWC is small compared with that of HD ( $\sim 10\%$ ) [9]. Thus, the estimated amount of  $D_{\text{pumped}}$  in the measurements would have about 10% error-bars.

The H removal rate of pure He ICWC is about  $10^{17}$  H/sec, which is less than 10 % of that in GDC (see Table 4).

Figure 2 b) shows an example of the water removal by inter-shot ICWC. During the 2<sup>nd</sup> campaign, water was the dominant impurity through the campaign with an average percentage of about 7 %. Without Inter shot ICWC, the water pressure increases rapidly in several hours up to  $1.5 \times 10^{-8}$  mbar. The increase of the water pressure is effectively suppressed by inter-ICWC.

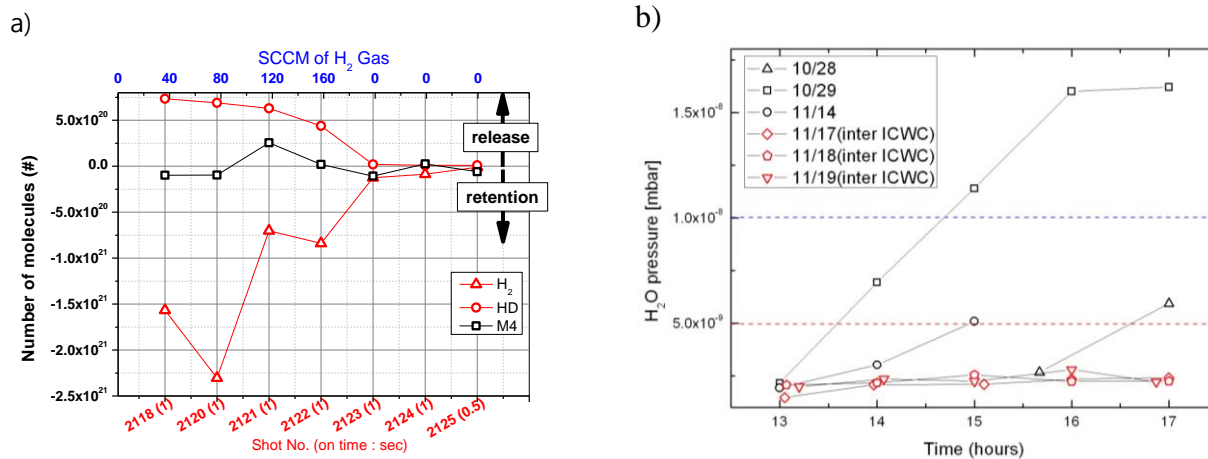


Figure 2. a)  $H_2$  and HD depending on  $H_2$  mixture rate. b) water removal by inter-shot ICWC during the campaign (x-axis label represent the time during the day). The dotted lines are guide to the eye.

### 3.4. Boronization

Figure 3 shows mass spectra of  $H_2O$  (solid line) and  $H_2$  (dashed line) for two successive days before and after the boronization. A large drop of  $H_2O$  level ( $-\Delta H_2O$ ) by a factor of 10, and the increase of  $H_2$  level ( $+\Delta H_2$ ) by a factor of 3 can be seen after the boronization.

Normalized intensity (divided by  $n_e$ ) of filterscope measurements for OII and CIII at outer wall were decreased by a factor of 2 (OII and CIII) after the boronization (not shown here). Emission spectroscopy indicates also an increase of BII (345 nm) peak after the boronization, which decreases as a function of time, while OII (441.5 nm) and CIII (464.7 nm) intensities decrease, then increase as a function of time (not shown here). The lifetime of a-C/B:H layers was about 100 shots.

The quality of deposited boron thin film has to be investigated to improve oxygen gettering efficiency and hydrogen contents in the layers. The thin film deposited on stainless steel coupons installed just below the carborane injection port was about 180 nm with a complex refractive index of  $n=2.34$  and  $k=0.25$  @ 632 nm, which is very similar to that of a hard diamond-like carbon film [11]. Since the XPS analysis shows that thin film has a relatively small fraction of boron (maximum about 3 %), the deposition was dominated by hydrocarbons. Using the fact that the complex refractive of an a-C:H film is directly related to the hydrogen to carbon ratio and the density of the material [12], the deposited film has 25-30 % of H/H+C ratio and a density of about  $2.0\text{-}2.2 \text{ g cm}^{-3}$ . A direct SIMS measurements show similar results.

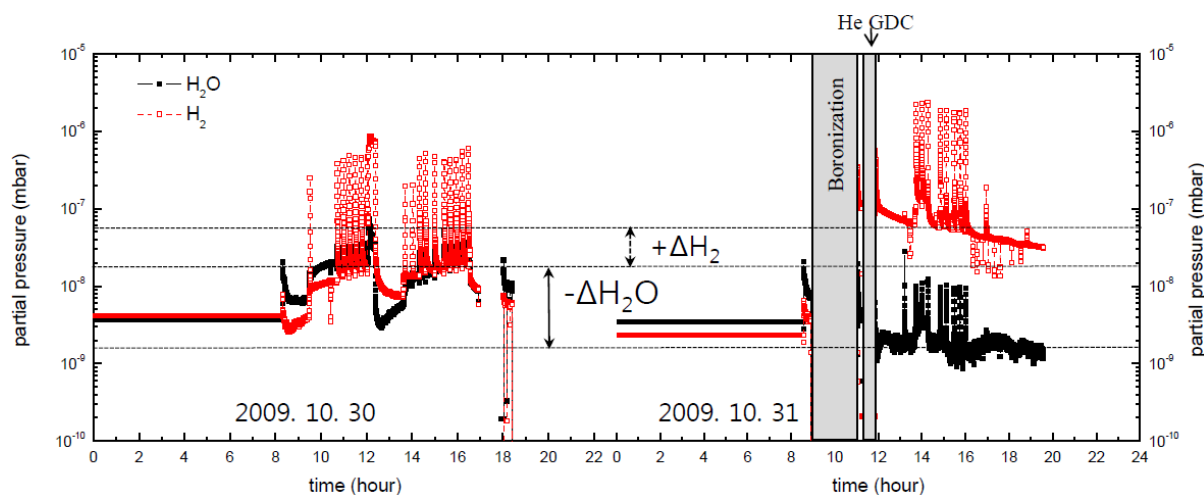


Figure 3. Mass spectra of  $\text{H}_2\text{O}$  (closed square) and  $\text{H}_2$  (open square) for two successive days before and after the boronization.

#### 4. Summary and Conclusion

In this paper, initial phase wall conditioning in KSTAR is described. After the series of wall conditioning procedures, a better wall condition is achieved.

The outgassing rate per unit area in the vacuum vessel was significantly reduced by baking.

The operational windows for GDC have been scanned and the optimization is underway. In a He GDC, a particle removal rate of  $\sim 10^{18}\text{-}10^{19}$  particle/sec is obtained while that of ICWC is  $\sim 10^{17}\text{-}10^{18}$  particle/sec.  $H_{\text{implanted}}/D_{\text{pumped}}$  during the ICWC is about 5-15. Pulsed operation seems more effective than CW. From the observation by in-vessel TV system, it seems that the cleaning is effective at low field side out-board. Also, the homogeneity of the plasma has to be improved by applying external poloidal magnetic fields. The ICWC results are consistent with that from other machines.

First boronization in KSTAR was successfully performed by using carborane vapor. Water

and oxygen level in vacuum vessel have been reduced significantly. However, additional H atoms dissociated from carborane mother molecule would be a small problem for the density control during a following shot. Boron containing thin films deposited by boronization are hard diamond-like films with small amount of boron components with a density of 2.0-2.2 g/cm<sup>3</sup>, H/H+C ratio of 25-30 %.

### Acknowledgements

\* This study is supported by the Korean Ministry of Education, Science and Technology under the KSTAR project (No. 2009-0082706 and No. 2010-0020044 )

### References

- [1] J. Winter, *Plasma Phys. Controlled Fusion*, 38 (1996) 1503-1542
- [2] G. Federici et al., *Nucl. Fusion*, 41 (2001) 1967-2137
- [3] K.M. Kim, H.L. Yang, S.H. Hong, S.T. Kim, H.T. Kim, K.P. Kim, K.S. Lee, H.K. Kim, J.S. Bak and KSTAR team, *Fusion Engineering and Design*, **84** (2009), 1026-1028
- [4] Y. D. Bae et al., *Nucl. Fusion* 43 (2003) 805-811
- [5] S.H. Hong, K.S. Lee, K.M. Kim, H.T. Kim, G.P. Kim, J.H. Sun, H.J. Woo, J.M. Park, W.C. Kim, H.K. Kim, K.R. Park, H.L. Yang, H.K. Na, K.S. Chung and KSTAR team, *Fusion Engineering and Design*, Article in Press, doi:10.1016/j.fusengdes.2010.04.064
- [6] V. M. Sharapov et al., *Journal of Nuclear Materials* 220-222 (1995) 730-735
- [7] J. Li et al., *Nuclear Fusion*, Vol. 39, No. 8 (1999) 973
- [8] X. Gao et al., *J. Nucl. Mater.* 390-391 (2009) 864-868
- [9] D. Douai, T. Wauters, S. Bremond, E. de la Cal, G. Lombard, A. Lyssoivan, B. Pergourie, E. Tsitrone, and Tore Supra Team, Special Expert Working Group on Fuel Removal, 16. June. 2009
- [10] Private communication, 12<sup>th</sup> ITPA Div/SOL group meeting report
- [11] S. H. Hong, Ph.D. thesis, 2004, Ruhr-University Bochum, Germany.
- [12] T. Schwarz-Selinger, A. von Keudell, and W. Jacob, *J. Appl. Phys.*, Vol. 86, No. 7, 1 October 1999